

Application of hydrogen-bond propensity calculations to an indomethacin–nicotinamide (1:1) co-crystal

Article

Accepted Version

Majumder, M., Buckton, G., Rawlinson, C. F., Williams, A. C. ORCID: <https://orcid.org/0000-0003-3654-7916>, Spillman, M. J., Pidcok, E. and Shankland, K. (2013) Application of hydrogen-bond propensity calculations to an indomethacin–nicotinamide (1:1) co-crystal. *CrystEngComm*, 15. pp. 4041-4044. ISSN 1466-8033 doi: <https://doi.org/10.1039/c3ce40367j> Available at <https://centaur.reading.ac.uk/32474/>

It is advisable to refer to the publisher's version if you intend to cite from the work. See [Guidance on citing](#).

To link to this article DOI: <http://dx.doi.org/10.1039/c3ce40367j>

Publisher: Royal Society of Chemistry

All outputs in CentAUR are protected by Intellectual Property Rights law, including copyright law. Copyright and IPR is retained by the creators or other copyright holders. Terms and conditions for use of this material are defined in the [End User Agreement](#).

www.reading.ac.uk/centaur

CentAUR

Central Archive at the University of Reading

Reading's research outputs online

Cite this: DOI: 10.1039/c0xx00000x

www.rsc.org/xxxxxx

Application of hydrogen-bond propensity calculations to an indomethacin-nicotinamide (1:1) co-crystal†

Mridul Majumder,^{a,b} Graham Buckton,^c Clare F. Rawlinson-Malone,^d Adrian C. Williams,^b Mark J. Spillman,^b Elna Pidcock^e and Kenneth Shankland^{d,b}

Received (in XXX, XXX) Xth XXXXXXXXXX 20XX, Accepted Xth XXXXXXXXXX 20XX

DOI: 10.1039/b000000x

The crystal structure of an indomethacin-nicotinamide (1:1) co-crystal produced by milling has been determined from laboratory powder X-ray diffraction (PXRD) data. The hydrogen-bonding motifs observed in the structure represent one of the most probable of all the possible combinations of donors and acceptors in the constituent molecules.

Indomethacin (IND; Fig 1) and nicotinamide (NIC; Fig 1) are well-known co-crystal formers,¹ and an IND:NIC (1:1) co-crystal has been reported and its physicochemical properties characterised.² A recent 2D solid-state magic-angle spinning NMR study³ has identified a strong $N_{\text{arom}} \cdots \text{HOOC}$ hydrogen bond (H-bond) but the crystal structure has not been reported. This communication describes the crystal structure of IND:NIC, as solved directly from laboratory-based PXRD data, and a full H-bonding propensity analysis of the IND and NIC molecules.

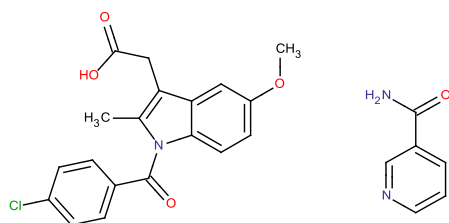


Fig. 1 The molecular structures of IND (left) and NIC (right).

A 1:1 molar ratio mixture of IND-MeOH solvate⁴ and NIC was milled in a ball mill for ca. 4 hrs. During the milling process, the mixture desolvated, leading to co-crystal formation. The resultant material was loaded into a 0.7mm borosilicate glass capillary and transmission PXRD data collected at room temperature. ‡ The diffraction pattern indexed to a monoclinic unit cell of volume 2343 \AA^3 , indicative of a 1:1 IND:NIC co-crystal. A Pawley-type refinement of the unit cell parameters in space group $P2_1/c$ was carried out using TOPAS,⁵ yielding a fit with $R_{\text{wp}} = 1.236$. The crystal structure was then solved using DASH⁶ and the structure refined against the original data using TOPAS. ¶ The final refinement included a total of 44 parameters (21 background, 1 scale, 6 torsions, 3 angles, 6 position, 6 orientation and 1 non-H ITF), yielding $R_{\text{wp}} = 2.912$.

The resulting structure was further scrutinised by allowing all

fractional coordinates to refine freely. As expected, the reduction in R_{wp} to 1.569 came at the expense of some chemical sense (mainly H-atom positions), but otherwise the geometry of each of the two molecules was well preserved. The NIC molecules form H-bonded chains which interact with the carboxylic acids of neighbouring IND molecules via H-bonding of the amide and N_{arom} functional groups.

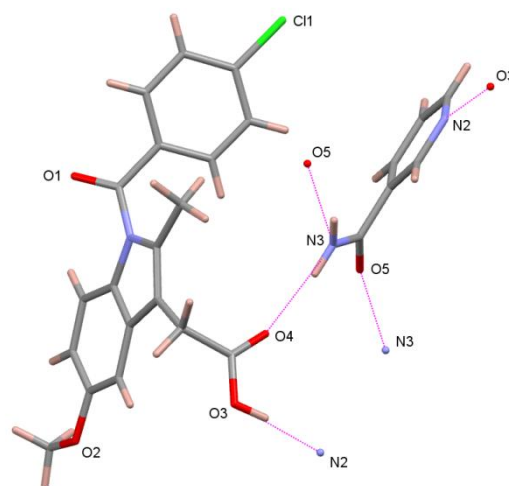


Fig. 2 H-bonding scheme in the 1:1 IND:NIC crystal structure.

In order to place the observed H-bonding interactions in the context of the possible interactions that can occur between IND and NIC, H-bond propensities were calculated⁷ using the program Mercury 3.1.⁸ Briefly, an H-bond propensity is determined from a statistical model built for each donor and acceptor pair. The training dataset for the statistical models is composed of molecules extracted from the Cambridge Structural Database⁹ (CSD) that contain between one and all of the functional groups present in the target system. Variables describing the environment of the functional group (e.g. steric density, aromaticity and competition) are recorded for each functional group along with the presence or absence of an H-bond between the functional groups. A logistic regression is applied to the training dataset which allows, upon consideration of the environmental variables for the functional groups of the target molecule(s), predictions in the form of H-bond propensities to be determined. An H-bond propensity for a donor-acceptor pair can

take a value between 0 and 1, where 0 indicates no likelihood of H-bond formation and 1 indicates that an H-bond will always be found. For a co-crystal system, where two components A and B are present, an H-bond propensity calculation¹⁰ determines the likelihood of H-bonding interactions of A with A, B with B and A with B. This methodology can be used to direct co-crystal screening experiments by providing a quantitative measure of the likelihood of an interaction between the two components of the system. Alternatively, it can be used to assess observed co-crystal structures. An observed H-bonding pattern composed of interactions of high propensity is in accord with expectations derived from the body of information in the CSD and hence can be thought of as favourable. Conversely an observed H-bond pattern that includes unusual outcomes raises an interesting question with regard to favourability: might there be other, more favourable H-bond patterns displayed in polymorphs that are as yet undiscovered by screening experiments?

The functional groups defined for the purpose of the H-bond propensity calculation (Fig 3) were taken from the library of functional groups provided with the software and the results of the H-bond propensity calculation performed on the IND:NIC system are given in Table 1.

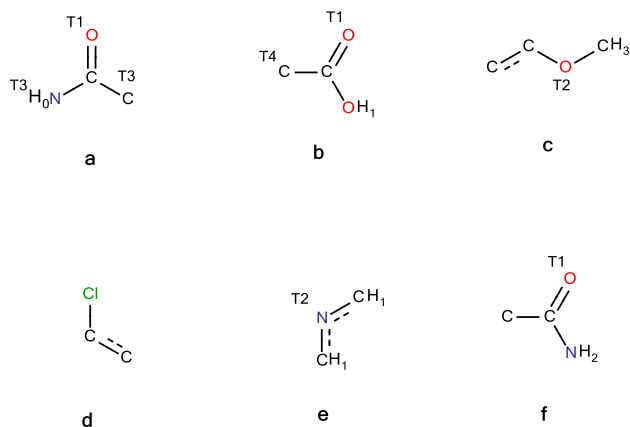


Fig. 3 Functional group definitions for the IND/NIC co-crystal system. Atom super-script labels, Tx, enumerate the coordination number of the specified atoms. Aromatic bond types are shown with a dashed and solid line combination. The functional groups defined are a) carbonyl (**O1**), b) carboxylic acid (**O3**, **O4**), c) methoxy (**O2**), d) aryl chloride (**Cl1**), e) pyridine (**N2**) and f) amide (**N3**, **O5**). Note that the bracketed atom identifiers given in bold correspond with those used in Fig. 2. The combinations of these functional groups are summarised in Table 1 and in the ESI.

It can be seen that the NIC-NIC amide chain is predicted to occur with a high propensity, as is the interaction between the NH₂ group of the amide and the carboxylic acid group of IND (interactions 1 and 3 in Table 1). The final H-bond interaction observed in the crystal structure is the donation of the IND acidic proton to the aromatic nitrogen of NIC (interaction 5 in Table 1). Interactions 1 and 2 are observed in both polymorphs of nicotinamide.¹¹ In the IND:NIC crystal structure, donation of the NH₂ group to the IND carboxylic acid group is predicted to be competitive and the acidic proton of IND is able to satisfy the pyridine group. The C=O group of the amide is unlikely to accept twice and hence the "weaker" OH donation to the C=O of

the amide (interaction 4; Table 1) does not perturb interaction 1.

Table 1 Summary of the H-bond propensity calculation for the IND:NIC co-crystal, including lower (LB) and upper bounds (UB). The final column indicates if the interaction listed is observed in the crystal structure. The donor and acceptor groups are shown in Fig. 3.

Interaction	Donor	Acceptor	Propensity	LB	UB	
1	N3	O5	0.71	0.63	0.78	✓
2	N3	N2	0.70	0.61	0.77	
3	N3	O4	0.67	0.60	0.73	✓
4	O3	O5	0.59	0.51	0.67	
5	O3	N2	0.57	0.48	0.65	✓
6	O3	O4	0.54	0.48	0.60	
7	N3	O1	0.48	0.37	0.58	
8	O3	O1	0.35	0.27	0.44	
9	N3	O3	0.15	0.09	0.22	
10	N3	O2	0.13	0.08	0.19	
11	O3	O3	0.09	0.06	0.14	
12	O3	O2	0.08	0.05	0.11	
13	N3	Cl1	0.05	0.03	0.08	
14	O3	Cl1	0.03	0.02	0.05	

A further result of the H-bond propensity calculation is a chart (Fig 4) that displays possible combinations of donors and acceptors and ranks those combinations on the coordination environment of the functional groups (y-axis) and the propensity of the interaction (x-axis). This chart provides a landscape of permutations, with donor – acceptor combinations varying from less favourable (top left) to more favourable (bottom right). It is clear that the IND:NIC structure (pink dot) possesses one of the best permutations of donors with acceptors.

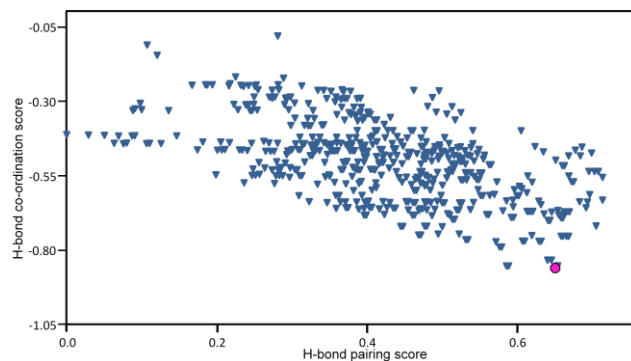


Fig. 4 A chart showing possible permutations of donors with acceptors for the IND:NIC system (blue triangles). The y axis plots the negative of the average coordination score whilst the x axis plots the average H-bond propensity score for the permutation. The observed structure is found to map onto the permutation highlighted with a pink circle. Optimal outcomes (high propensity score and high coordination score) are found in the bottom right of the chart.

Conclusions

One potential application of H-bond propensity calculations lies in the selection of likely co-formers for co-crystals, but it is clear from this study that applying such a calculation to a structure solved from powder diffraction can provide an informatics-based piece of evidence to support or oppose the hypothesis that the

Rietveld refinement global minimum has been correctly located. As the complexity of crystal structures solved from powder diffraction data increases, so does the likelihood of small structural ambiguities that may not be easily resolved from consideration of the fit to the diffraction data alone; in such cases, additional evidence to support a structure from either DFT-type calculations,¹² H-bond propensity considerations or similarity relationships¹³ is extremely valuable. In the case of the relatively simple IND:NIC co-crystal structure, H-bond propensity highlights the fact that the observed H-bonding scheme is one of several that are predicted to be favourable. It is possible that novel IND:NIC polymorphs could be found that exhibit these alternative favourable H-bonding schemes.

The crystal structure determination reported here was relatively straightforward. For more complex structures, it is possible that information returned by an 'a priori' H-bond propensity search could be incorporated into the crystal structure solution stage, in order to increase the probability of locating the global minimum.

Acknowledgements

We gratefully acknowledge the support of the STFC Centre for Molecular Structure and Dynamics for part-funding of MJS and the University of Reading Chemical Analysis Facility for access to powder diffraction facilities. We thank Dr. Norman Shankland for useful comments and discussions.

Notes and references

^a *Pharmaterials Ltd., Unit B, 5 Boulton Road, Reading RG2 0NH, UK. Fax: +44 (0) 1189 310679; Tel: +44 (0) 1189 209900; E-mail: mridul.majumder@pharmaterials.co.uk*

^b *School of Pharmacy, University of Reading, Whiteknights, Reading RG6 6AD, UK.*

^c *UCL School of Pharmacy, 29-39 Brunswick Square, London WC1N 1AX, UK.*

^d *Bristol-Myers Squibb Pharmaceuticals Limited, Reeds Lane, Moreton, CH46 1QW, UK.*

^e *Cambridge Crystallographic Data Centre, 12 Union Road, Cambridge, CB2 1EZ, UK.*

† Electronic Supplementary Information (ESI) available: Profile fits from Rietveld refinement and illustrations of the motifs enumerated in Table 1.

∇ The International Nonproprietary Name for indometacin is indometacin.

‡ PXR D data were collected over the range 4–80° 2θ (2 kW; Cu Kα₁, 1.54056 Å; step size 0.017° 2θ), using a variable count time scheme. The Bruker D8 Advance diffractometer was equipped with a LynxEye detector.

¶ The data set was background subtracted and truncated to 38.9° 2θ for Pawley fitting in DASH ($\chi^2=2.96$). The simulated annealing component of DASH was used to optimise the positions, orientations and conformations of molecular models of NIC (derived from CSD refcode GOGQID, with 7 DoF) and IND (derived from CSD refcode INDMET03, with 10 DoF) against the diffraction data (194 reflections), yielding a favourable χ^2 of 21.0 for the best solution. A TOPAS-type rigid-body description of this solution was then refined against the original data set in the range 4–80° 2θ to give a good final fit, $R_{wp}=2.912$, $R_e=1.153$. For the rigid-body refined fractional coordinates, with errors calculated by the bootstrap method, see CCDC reference number 926162.

§ The propensity score for each possible combination of donors and acceptors is calculated from the average of the contributing propensity scores. Similarly the coordination score is the average of the coordination scores that contribute to the particular permutation of donors and

acceptors. Coordination scores are calculated using a statistical model which captures the likelihood that a functional group participates 0, >1, >2 times.

1. S. Basavoju, D. Boström and S. Velaga, *Pharmaceutical Research*, 2008, 25, 530-541; M. Majumder, G. Buckton, C. Rawlinson-Malone, A. C. Williams, M. J. Spillman, N. Shankland and K. Shankland, *Crystengcomm*, 2011, 13, 6327-6328; L. Padrela, M. A. Rodrigues, S. R. Velaga, H. A. Matos and E. G. de Azevedo, *Eur. J. Pharm. Sci.*, 2009, 38, 9-17; S. Ando, J. Kikuchi, Y. Fujimura, Y. Ida, K. Higashi, K. Moribe and K. Yamamoto, *J. Pharm. Sci.*, 2012, 101, 3214-3221; L. Fabian, N. Hamill, K. S. Eccles, H. A. Moynihan, A. R. Maguire, L. McCausland and S. E. Lawrence, *Cryst. Growth Des.*, 2011, 11, 3522-3528; S. G. Fleischman, S. S. Kuduva, J. A. McMahon, B. Moulton, R. D. B. Walsh, N. Rodriguez-Hornedo and M. J. Zaworotko, *Cryst. Growth Des.*, 2003, 3, 909-919; J. Lu and S. Rohani, *Org. Process Res. Dev.*, 2009, 13, 1269-1275; J. F. Remenar, M. L. Peterson, P. W. Stephens, Z. Zhang, Y. Zimenkov and M. B. Hickey, *Mol. Pharm.*, 2007, 4, 386-400.
2. A. Alhalaweh, A. Sokolowski, N. Rodriguez-Hornedo and S. P. Velaga, *Cryst. Growth Des.*, 2011, 11, 3923-3929; A. Alhalaweh and S. P. Velaga, *Cryst. Growth Des.*, 2010, 10, 3302-3305.
3. K. Maruyoshi, D. Iuga, O. N. Antzutkin, A. Alhalaweh, S. P. Velaga and S. P. Brown, *Chemical Communications*, 2012, 48, 10844-10846.
4. K. J. Crowley and G. Zografi, *J. Pharm. Sci.*, 2002, 91, 492-507.
5. A. A. Coelho, *TOPAS User Manual*, Bruker AXS GmbH, Karlsruhe, Germany, 2003.
6. W. I. F. David, K. Shankland, J. van de Streek, E. Pidcock, W. D. S. Motherwell and J. C. Cole, *J. Appl. Crystallogr.*, 2006, 39, 910-915.
7. P. T. A. Galek, L. Fabian, W. D. S. Motherwell, F. H. Allen and N. Feeder, *Acta Crystallographica Section B*, 2007, 63, 768-782.
8. C. F. Macrae, I. J. Bruno, J. A. Chisholm, P. R. Edgington, P. McCabe, E. Pidcock, L. Rodriguez-Monge, R. Taylor, J. van de Streek and P. A. Wood, *J. Appl. Crystallogr.*, 2008, 41, 466-470.
9. F. Allen, *Acta Crystallographica Section B*, 2002, 58, 380-388.
10. A. Delori, P. T. A. Galek, E. Pidcock and W. Jones, *Chemistry – A European Journal*, 2012, 18, 6835-6846; P. T. A. Galek, E. Pidcock, P. A. Wood, I. J. Bruno and C. R. Groom, *Crystengcomm*, 2012, 14, 2391-2403; A. Delori, P. T. A. Galek, E. Picock, M. Patni and W. Jones, *Crystengcomm*, 2013, in press.
11. W. B. Wright and G. S. D. King, *Acta Crystallographica*, 1954, 7, 283-288; J. Li, S. A. Bourne and M. R. Cairra, *Chemical Communications*, 2011, 47, 1530-1532.
12. J. van de Streek and M. A. Neumann, *Acta Crystallographica Section B*, 2010, 66, 544-558.
13. T. Gelbrich and M. B. Hursthouse, *Crystengcomm*, 2005, 7, 324-336.